

# Simulation of LNG-Battery Hybrid Tugboat Under the Influence of Environmental Loads and Manoeuvre

Sharul Baggio Roslan<sup>1</sup>, Dimitrios Konovessis<sup>2</sup>, Joo Hock Ang<sup>3</sup>, Nirmal Vineeth<sup>3</sup> and Zhi Yung Tay<sup>1,\*</sup>

## ABSTRACT

*This paper presents a system modelling approach aimed at designing and simulating real-time conditions, with a specific focus on extreme scenarios to assess the impact on the annual CO<sub>2</sub> emissions and the consumption of LNG and batteries in a hybrid tugboat. Environmental variables such as wave period, wave height, current speed, and wind speed are considered. The tugboat system model is validated using manually logged historical operational data from a similar tugboat profile using both AMESIM and MATLAB\Simulink to simulate diverse environmental conditions and estimate annual fuel operational costs and emissions. A comparative analysis of the different system configurations is then conducted between traditional diesel, LNG and several control configurations of LNG-battery hybrid. Results demonstrate a significant reduction of 96.5% in CO<sub>2</sub> emissions and a 95.3% decrease in annual fuel operational costs with the adoption of LNG-battery hybrid propulsion with the rule-based control system. The study notes a slight increase in vessel operational time by 10.8% due to higher wave heights and a 0.97% rise in added resistance from increased wind speed. Insignificant differences are observed in variations of wave period and current speed. Additionally, the CII ratings of the different system configurations were then compared and concluded with the LNG-battery hybrid with a rule-based control system being the most environmentally and economically sustainable.*

## KEYWORDS

Hybrid Marine Power System; LNG; Hybrid Tugboat; Energy Efficiency Operation Index; Carbon Intensity Indicator; System Modelling; System Optimisation; Control Strategies; Rule-Based Control; Energy Management System; Carbon Emissions; Fuel Cost

## 1. INTRODUCTION

Given Singapore's standing as home to one of the world's busiest ports, addressing greenhouse gas (GHG) emissions has become a top priority. The Marine Port Authority (MPA) targets ensuring that by 2030, all newly commissioned harbor vessels operating within Singapore's port waters will either be entirely electric, have the capacity to utilise B100 biofuel or be compatible with net-zero fuels like hydrogen. Vessel owners are mandated to collaborate with MPA on these designs by 2027 (Maritime & Port Authority Of Singapore, 2023). The MPA's initiative serves as a strategy to ready operational vessels for compliance with the MARPOL Annex VI, established by the International Maritime Organization (IMO) in 2016, aiming to halve annual GHG emissions by 2050 (International Maritime Organization, 2016), with an intermediate target of a 40% reduction by 2030 and an even more substantial 70% reduction by 2050. Additionally, stringent emissions limits, such as the 0.5% m/m marine sulfur content limit in emission-controlled areas (ECA) implemented in January 2020 (International Maritime Organisation, 2019), have necessitated vessel owners to explore diverse methods to curtail CO<sub>2</sub> emissions (Tadros *et al.*, 2023). This includes the adoption of scrubbers/exhaust gas clearing systems, carbon capture and storage, or net-zero fuel sources like

---

<sup>1</sup> Singapore Institute of Technology (Engineering, Singapore Institute of Technology, Singapore); ORCID: 0009-0007-4642-2216

<sup>2</sup> National Technical University of Athens (School of Naval Architecture and Marine Engineering, Athens, Greece); ORCID: 0000-0003-0085-4690

<sup>3</sup> Seatrium Limited (Seatrium Limited, Singapore)

\* Corresponding Author: zhiyung.tay@singaporetech.edu.sg; ORCID: 0000-0003-3194-1965

hydrogen, ammonia, or LNG (Mallouppas & Yfantis, 2021). With the various results from reducing emissions, the results are then assessed based on two new indexes introduced by the 76<sup>th</sup> Marine Environment Protection Committee (MEPC) (The Marine Environment Protection Committee, 2021). The Efficient Existing Ship Index (EEXI), the annual carbon intensity indicator (CII) operation report and the CII rating that was implemented in 2023. The EEXI applies to existing ships and requires these ships to fulfil the minimum energy efficiency standards, otherwise, the ship may need to implement technical and operational measures to improve its energy efficiency (ClassNK, 2021). CII ratings and annual CII operational reports are required for vessels of more than 5,000. CII ratings are based on the ship's CO<sub>2</sub> emissions during an operation, achieving a grade "A" CII rating signifies a highly efficient ship in reducing carbon emissions during operation. Ships with a rating of "D" or "E" for three consecutive years are required to develop a corrective action plan. A past study by Ejder and Arslanoğlu (2022) on CII explored using ammonia fuel engines, identifying potential savings of 12,660.07 tonnes of CO<sub>2</sub> and achieving an 'A' CII rating. However, the \$5 million retrofitting cost makes building a new ship more economically viable. Another study by Gianni *et al.* (2022) assessed various power configurations for a cruise ship not meeting CII regulations. Only marine gas oil (MGO) failed to comply with the 2024 CII regulations, while LNG power was the sole option capable of securing an 'A' CII rating until 2026.

Given the urgent need to decrease GHG emissions, it is important to explore alternative solutions. Notably, there has been a surge in technological advancement and the widespread commercial adoption of electrical or hybrid propulsion in recent years. The earliest application of electrical propulsion in vessels existed since the 1990s, primarily used in military and cruise ships (Moreno, 2007) and the world's first electric-powered car ferry, the Ampere, was built later in 2015 (Ship Technology, 2015). The electrical propulsion system provides higher efficiency lower carbon emission or zero emission in low loading conditions (Tay & Konovessis, 2023), and overall reduces operational cost. Since LNG shrinks by a factor of 1/600 during liquification, it becomes easier to be transported around making it more accessible when compared to other alternative fuels, hybrid propulsion using natural gas-powered engines or batteries has also recently seen an increase in popularity (Roslan *et al.*, 2022). A few noteworthy research studies, including Vadset (2018) thesis which delved into LNG-powered systems. Vadset's research specifically explored LNG–battery hybrid systems, comparing those with variable speeds to full-LNG systems. The study revealed that a variable-speed LNG-battery system could achieve a 20% reduction in fuel costs compared to a fixed-speed fully LNG system. Another significant research from Lebedevas *et al.* (2021) conducted notable past research on the utilisation of LNG dual-fuel engines for tugboats. Their work achieved reductions of 10%, 91%, and 65% in CO<sub>2</sub>, SO<sub>2</sub>, and NO<sub>x</sub> emissions, respectively. Compared to utilising diesel, using a hybrid diesel-LNG propulsion system saves 33% on fuel costs. Moreover, LNG serves as a cost-efficient fuel with the potential to cut down CO<sub>2</sub> emissions by 26%, and it is sulphur-free, although the presence of methane slip may diminish its environmental advantages (Karaçay & Özsoysal, 2021). The authors are not aware of many studies focusing on the LNG–battery hybrid system, especially in the context of tugboats. This gap in research serves as the motivation for exploring this subject in the current paper.

In addition to enhancing emissions through the incorporation of renewable energy, it is important to explore ways to boost ship energy efficiency. This involves investigating the most optimised environmental conditions for optimal operation to achieve further reduction in emissions. Some noteworthy research on the impact of environmental factors on energy consumption has been conducted. A study done by Lindstad *et al.* (2013) revealed that a 4m head wave could increase energy consumption by up to 35%, while an 8m wave height might lead to a doubling of energy consumption for a bulk carrier. A study which explored different conditions of wind speed, wind direction and wave height conducted by Wang *et al.* (2023), managed to reduce fuel consumption by 3.38%. Currently, there is limited research employing system modelling on the impact of environmental loads on the performance and manoeuvrability of an LNG-battery hybrid system. This led to incorporating the topic into the current. While the selection of a route significantly influences a ship's efficiency, this paper specifically focuses on a fixed operational route. Future research is encouraged to explore route optimisation-based solutions based on the most efficient conditions discovered in this paper.

This study aims to evaluate the environmental and economic effects of adopting a LNG–battery hybrid propulsion system in a 65-ton tugboat in comparison to utilising diesel or LNG as the sole propulsion system. By utilizing data obtained from a comparable diesel-powered tugboat, the study profiles the loading operations of the modelled tugboat. The hybrid LNG–battery tugboat system is created in MATLAB/Simulink<sup>®</sup> and a diesel-powered tugboat is created in AMESIM, the full system breakdown is described in Section 2. The case study adopted for this study was obtained based on the design operational profile. Several different environmental conditions are tested to analyse the effects of varying environmental conditions on the engine load, annual fuel operation cost and annual CO<sub>2</sub> emissions emitted. Finally, an assessment was conducted to compare the CII rating of an LNG-battery hybrid system, employing rule-based control and various load distribution strategies, against conventional diesel and LNG systems. The goal was to identify the system with the best rating and economically and environmentally beneficial. Although CII ratings are not required for vessels below 5,000GT, this paper will neglect the weight requirements and categorise the tugboat as a cruise passenger ship for comparison purposes. The rule-based control and load distribution strategies adopted from this study are based on a past study conducted by the author (Roslan, Konovessis, *et al.*, 2023; Roslan, Tay, *et al.*, 2023). Further development of the system modelling could be conducted with the advancement of digital twins that incorporates machine learning (Abebe *et al.*, 2020; Cheliotis *et al.*, 2020; Fam *et al.*, 2022; Hadi *et al.*, 2022a; Tay, Z.Y.; Hadi, J; Konovessis, D.; Loh, D.J.; Tan, D.K.H; Chen, 2021; Tay *et al.*, 2021) and big data analytics (Hadi *et al.*, 2022b; Mirović *et al.*, 2018).

The paper is structured as follows: Section 2 provides an overview of the tugboat, details of the methodology for obtaining the vessel loading profile, and a brief description of both the diesel-powered tugboat system modelled on AMESIM and the hybrid LNG–battery power system modelled on Simulink. In Section 3, a mathematical overview is presented for the comparison study. Section 4 compares the annual operation cost and annual CO<sub>2</sub> emissions across different cases and configurations. Finally, Section 5 concludes with a summary of the work and provides recommendations for future research.

## 2. SYSTEM OVERVIEW

The diagrams of both the diesel and LNG-battery hybrid tugboats are shown in Figure 1 and Figure 2, respectively. Figure 1 shows the system diagram of a diesel tugboat. Operational data from JMS Kappa was acquired due to its resemblance in operational requirements and vessel architecture. The diesel tugboat is equipped with two diesel engine generators as a primary source, with a rated output of 1,471kW, and rated speed of 750rpm and a low output nominal voltage of 400V generator with a capacity of 1,390kWh for the auxiliary load (IHI, 2022). The auxiliary load includes service and hotel loads, heating, ventilation and air-conditioning (HVAC), lighting and pumps. The two diesel engines are then directly connected to a gearbox, to reduce engine speed and reversing shaft rotation. Subsequently, connected to an azimuth thruster individually. The diesel power system is modelled in Simcenter AMESIM to replicate the dynamic response of the system.

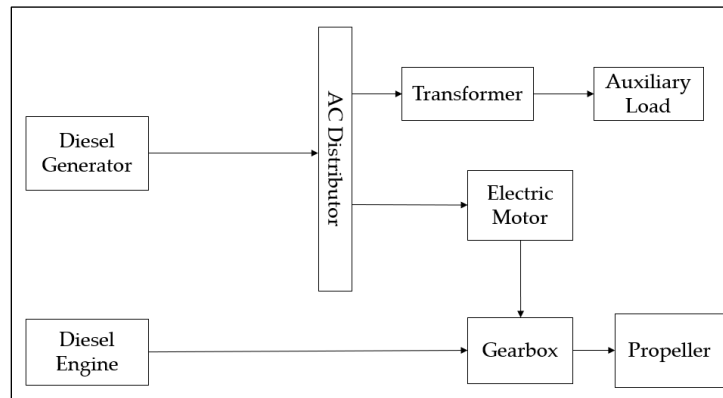


Figure 1. Simplified diagram of a diesel-electric vessel power system.

The tugboat's hybrid power system, shown in Figure 2, utilises two LNG generator sets (Gensets) with a maximum output of 1,492 kW, 1,600 rpm speed, and 545 V voltage for primary power generation. Additionally, two lithium-ion batteries, each with a 452 kWh capacity, provide energy storage. The vessel loads include the two azimuth thrusters with ducted propellers, service and hotel load, HVAC, lighting and pumps. A 1,000 V modern direct current (DC) distribution system is used in the present system due to its simplicity and fuel efficiency (Zahedi *et al.*, 2014). To streamline the system, AC power from the Gensets flows through a rectifier to become DC, while the battery directly feeds the DC distribution. This reduces equipment and boosts round-trip efficiency. The hybrid power system is modelled in MATLAB/Simulink® to simulate the dynamic response of the system.

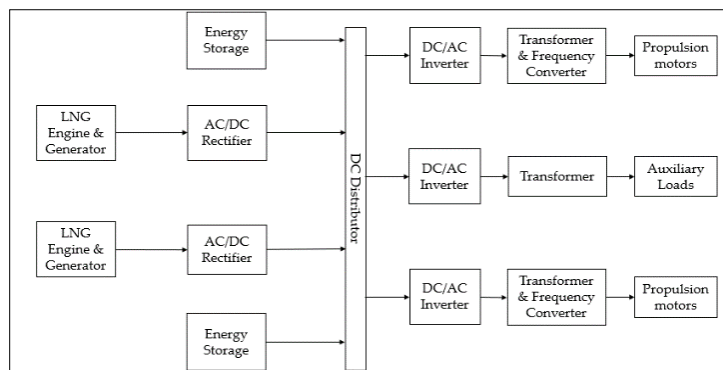


Figure 2. Diagram of LNG–battery hybrid vessel power system

### 2.1 Loading Profile

This study focuses on a 65-tonne tugboat equipped with two Gensets and batteries. The three primary operational modes categorised in this study are (i) idle or standby: in this mode, the vessel load ranges below 520kW and is either stationary or travelling along with the current. (ii) Transit: During transit, the speed and vessel load range between 6 - 12 knots 550kW and

1,100kW, respectively. (iii) Tugging: When performing tugging operations, the vessel load ranges up to a maximum load of 1,492kW, however, it averages 540kW with varying travelling speeds. The tugboat’s operational time-domain load profile was created based on past studies done by the authors (Roslan, Konovessis, *et al.*, 2023; Roslan, Tay, *et al.*, 2023), utilising a combination of data manually recorded during an operational on the diesel tugboat, JMS Kappa, and the designed operational profile of the LNG-hybrid tugboat provided by the industrial collaborators.

## 2.2 Modelling of Diesel Propulsion System on Simcenter AMESIM

The Simcenter AMESIM model of the diesel propulsion tugboat consists of two major parts, i.e., the diesel generator set (genset) and vessel resistance shown in Figure 3. The system model shown is based on combinations of examples found in the Simcenter AMESIM library, with the values reconfigured to suit the parameters of JMS Kappa.

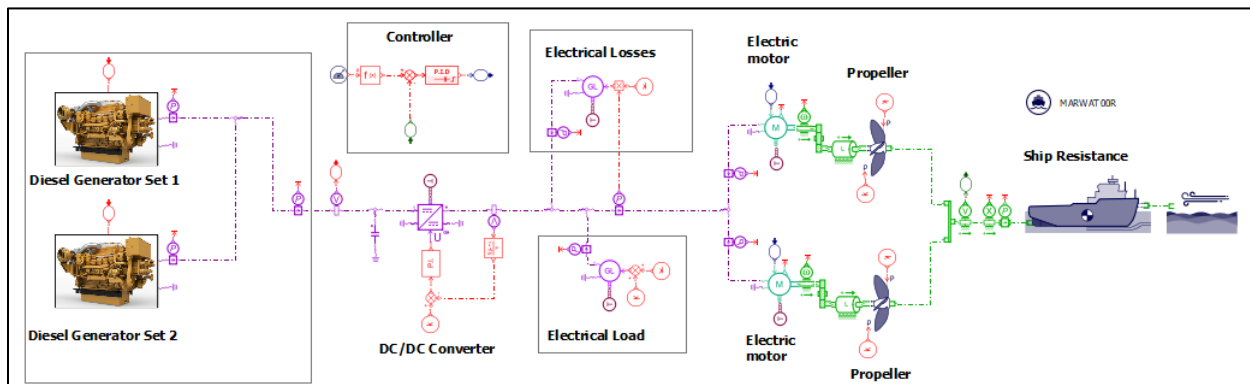


Figure 3. Model of the diesel power system in Simcenter AMESIM

### 2.2.1 Diesel Genset

The diesel engines are the main energy source for the diesel-powered tugboat. The generators are made up of diesel engines – DRVCE01H connected to electrical machines – DRVEMO3. The electrical generators then provide power through the DC/DC converter to two electrical motors that are connected to the propellers – MARPROP00, with a gear reduction system. The model also factors estimated auxiliary electrical load and electrical losses of 500kW and 0.5%, respectively. The parameters of the diesel genset – Niigata 6L26HLX, are based on the performance curves provided by the engine provider which are then replicated to the diesel engine model using the DRVCE table creator.

### 2.2.2 Vessel Resistance

The vessel resistance was based on CFD results shown in Figure 4, done on ANSYS Fluent and Finemarine with similar hull parameters to JMS Kappa. The results are then exploited and input into the vessel model, MARSHIP00, vessel resistance as a function of ship velocity. Speed ranging outside of the results provided are extrapolated linearly.

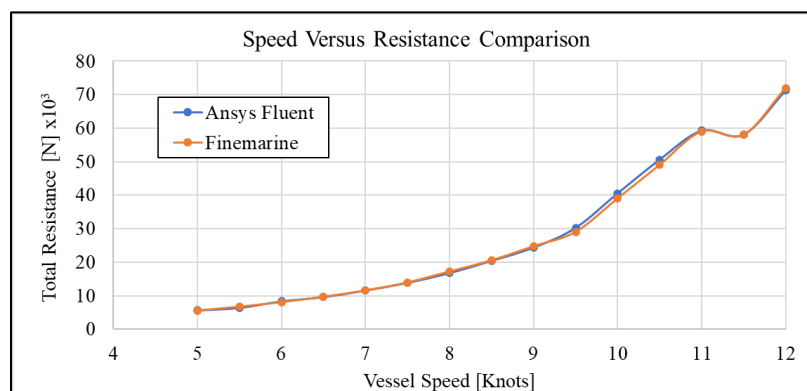


Figure 4. Vessel speed against resistance CFD results

The complete vessel route used in the study is shown in Figure 5, generated from the AMESIM Simcenter system simulation results and overlaid with Google Maps for easier visualisation. The operation observed in this study is based on data manually logged by the author during an operation. The route comprises segments of the tugboat cruising at high speed, tugging a vessel to an area near the shipyard and cruising back to the tugboat’s original dock. The return trip of the tugboat in the example used

is assumed to be travelling along the same route taken to travel out, in reality the tugboat operator may prefer to use alternative routes depending on the traffic or other operation demands. The load distribution is discussed in Section 4.

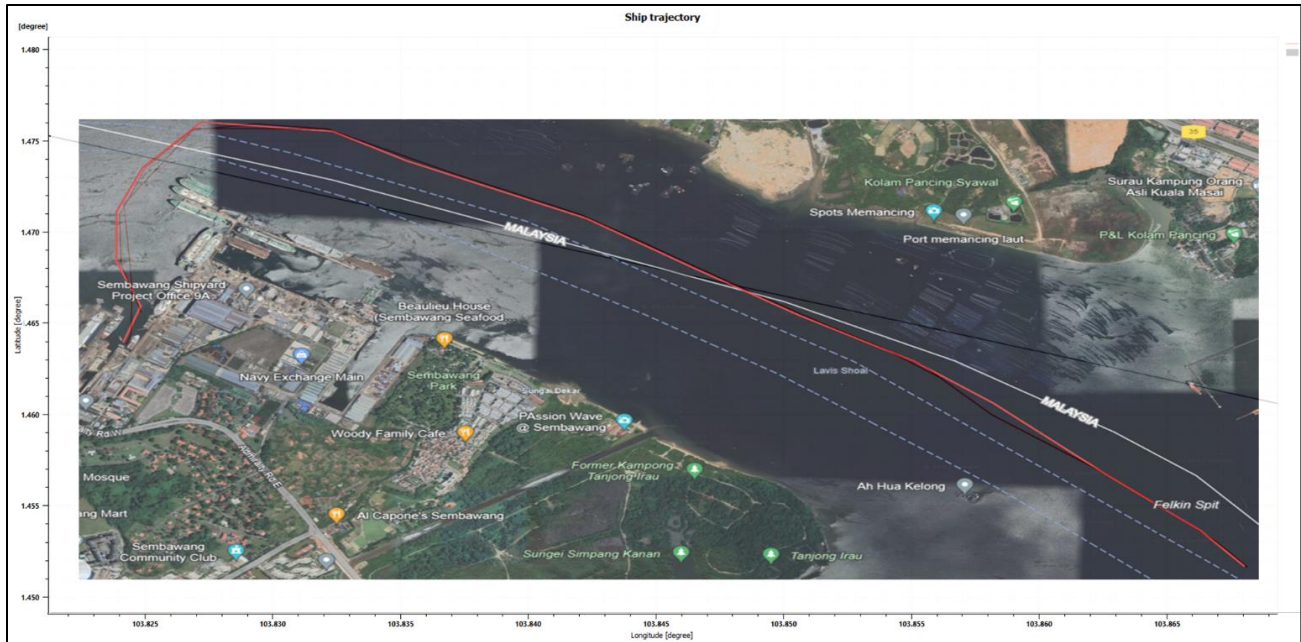


Figure 5. Vessel direction from Simcenter AMESIM results overlaid with Google maps

The environmental conditions during the specified route are based on several resources, i.e., the wave height is based on the MPA tide table (Maritime & Port Authority of Singapore, 2020) whereas the current speed and wind speed are based on data captured on a vessel with sensors capturing the current speed and wind speed along the similar route experience by the simulated vessel. The estimated average current speed and wind speed are also checked against online values from (Windfinder, 2020) for validation. These values along with the coordinates of the vessel operation route are then input into the marine environment model, MARWAT00R. The values used for this study are shown in Table 1. The added resistance due to the environmental conditions is computed through MARSEA00R using the Blendermann method and STAwave-2 for wind and wave resistance respectively. The Blendermann method is used to estimate the wind load based on wind tunnel test results and is one of the most accurate when compared to other methods such as the Isherwood and Gould method (Turk & Prpić-Oršić, 2009). STAwave-2 method is an empirical approach used to estimate the added resistance of a ship due to waves by STA-JIP (ITTC, 2021). The STAwave-2 is used due to its simplicity and one of the methods recommended by international standards (ISO, 2015). The controller in the system model - MARPOW00, determines the varying speed of the vessel during specific points of the operation.

Table 1. Parameters for MARWAT00R

Description	Value	Unit
Wind speed	2.21	m/s
Wave height	0.12	m
Current speed	0.387	m/s
Wave period	2.5	S
Water salinity	25	g/kg
Water temperature	30	°C

The control input table consists of the desired vessel speed at various coordinates during operation. It is noteworthy that the current system model is modelled with inputs from past operational data and not live data. Further development of the system modelling will be required to enable digital twinning of the system, where live data will be input instead. The system model's output incorporates diverse environmental factors and the vessel's added resistance to forecast the actual vessel speed, deviations in route, engine load requirements, added resistance, and estimated fuel consumption. The engine load results are subsequently compared with manually recorded data in Section 4 Case I. These findings are then used in the MATLAB/Simulink model detailed in the subsequent section to assess and compare the annual fuel operational costs and CO<sub>2</sub>

emissions associated with LNG-hybrid propulsion. The AMESIM model is then employed to examine how different environmental conditions impact vessel loading in Section 4 Case II.

### 2.3 Modelling of Hybrid LNG-Battery Propulsion System on MATLAB Simulink

The Simulink model for the hybrid system discussed in this paper follows a similar approach to that presented in (Roslan, Tay, *et al.*, 2023). However, this paper advances upon previous findings by incorporating operational condition results obtained from the AMESIM model. For a detailed explanation and parameters of the hybrid LNG-battery power system modelling using MATLAB/Simulink, readers are referred to (Roslan, Konovessis, *et al.*, 2023; Roslan, Tay, *et al.*, 2023). The LNG-hybrid model consists of three primary components: the Genset, the Gas Turbine (GAST), and the Battery, as illustrated in Figure 6. It is worth pointing out that the efficiency of the system components in both AMESIM and Simulink was assumed to be a constant of 90% and assumed that 10% is wasted due to heat. This assumption was made due to the lack of the component's efficiency curves. A system model that accounts for the efficiency curves of its components will be closer to real-world behaviour, important for digital twinning.

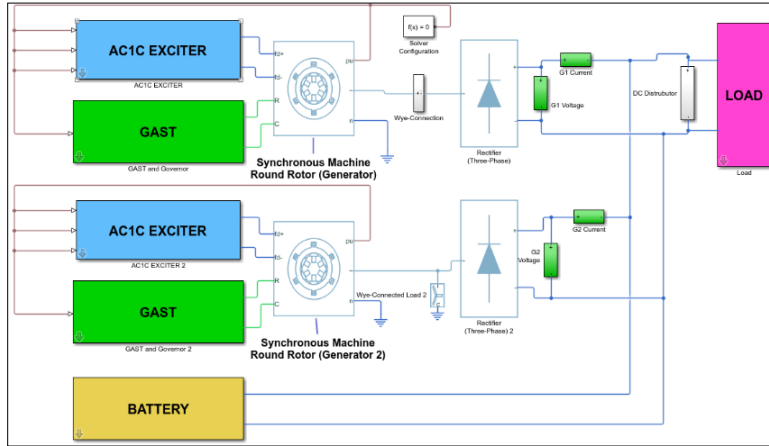


Figure 6. Model of Hybrid LNG-battery power system in Simulink.

### 2.4 Energy Management System

The energy management system (EMS) controls the different types of energy sources on board and fluctuating operational requirements. The optimal power distribution between the engine and energy storage system differs in the vessel fuel cost and emission emitted. To control and maintain the stability and distribution of the load required, a basic rule-based (RB) control strategy is added to the system model. The RB method is ideal with known loading conditions and past data of the system (Chua, 2019), where the past data are used as a benchmark for the RB control. This will then improve the power management of the hybrid system by allocating the different power sources efficiently to reduce operational costs and improve system longevity. The load-dependent RB control will be implemented in each case study similar to the one used in Roslan *et al.* (2023). The two types of RB strategy used in this paper are (1) LNG-RB: The Genset will be switched on/off to regulate the power switch to the fully battery-operated mode when the required load is consuming more than 200 g/kWh LNG or when each engine load of 300kW and below. (2) LNG/BAT: Based on the flexibility of the load sharing within the hybrid propulsions, different percentages of LNG and battery power in increments of 10% were investigated. A simple overview of the energy management framework is shown in Figure 7 below.

## 3. MATHEMATICAL OVERVIEW

### 3.1 Diesel Fuel Consumption

The calculation for diesel consumption is based on the method proposed by Hansen (2000) with some variations to accommodate the different systems. The mean specific fuel oil consumption ( $\overline{SFOC}$ ) could be obtained from the specific fuel oil consumption ( $SFOC$ ) for each Genset given in the diesel engine fuel consumption graph as follows,

$$\overline{SFOC} = \frac{1}{2t} \int_0^t [SFOC_{Gen_1}(t) + SFOC_{Gen_2}(t)] dt \quad (1)$$

where  $t$  is the total duration and the subscript in (1) denotes the  $SFOC$  for the respective Genset.

The  $\overline{SFOC}$  is then used to calculate the mean diesel consumption using the average generator power ( $P_{Avg}$ ). The mean diesel consumption  $\overline{C}_{diesel}$  calculation is shown in Equation (2).

$$\bar{C}_{diesel} [kg/h] = \overline{SFOC} [g/kWh] \times P_{Avg} [kW] \times 1000 \quad (2)$$

Note that the brackets in the equations represent the units for the variables and all the cost is in USD. The annual operation cost  $Cost_{annual}$  given in (3) is then calculated by taking the assumed diesel price  $P_{diesel}$ . As of writing, the average price of marine diesel oil is set to be USD 1.023/kg (Ship&Bunker, 2023).

$$Cost_{annual} [USD] = \bar{C}_{diesel} [kg/h] \times P_{diesel} [USD/kg] \times 24h \times 365 \quad (3)$$

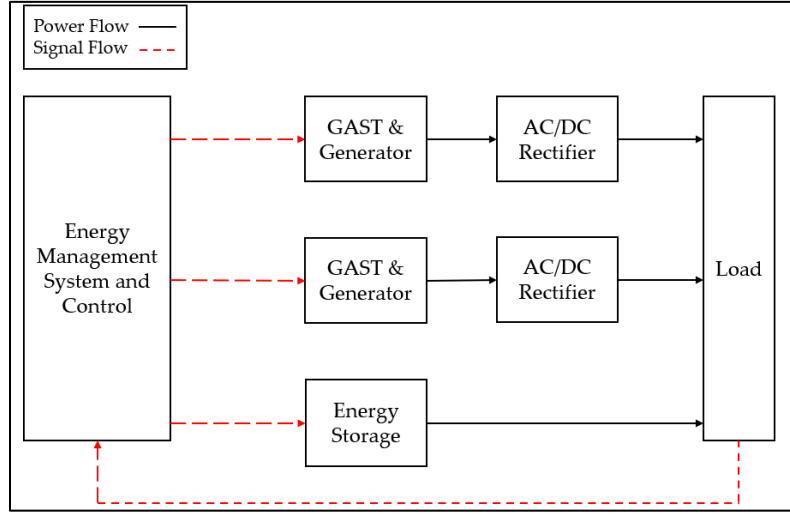


Figure 7. Simplified energy management framework (Roslan *et al.*, 2022)

### 3.2 LNG Consumption

For the LNG calculations, a similar concept to the diesel fuel counterpart is implemented. The mean LNG consumption  $\bar{C}_{LNG}$  is directly calculated from the summation of the  $SGC$  at the active load obtained from the engine limit curve in Figure 4.

$$\bar{C}_{LNG} \left[ \frac{Kg}{h} \right] = P_{Avg} [kW] \times \frac{1}{1000(2t)} \times \int_0^t \{SGC_{Gen 1}(t) + SGC_{Gen 2}(t)\} dt \left[ \frac{g}{kWh} \right] \quad (4)$$

The annual operation cost of the LNG is given in (5). The price of LNG  $P_{LNG}$ , as of writing, is set to be USD 0.40/kg (IndexMundi, 2022).

$$Cost_{annual} [USD] = \bar{C}_{LNG} [kg/h] \times P_{LNG} [USD/kg] \times 24h \times 365 \quad (5)$$

### 3.3 Battery Consumption

The battery consumption for the example will be calculated based on the difference in the battery state of charge (SOC). Using the Coulomb counting method (Vadset, 2018) given in (6),

$$SOC(t) = SOC(t-1) + \int_0^t \frac{P [kW]}{E_{bat} [kWh]} dt \quad (6)$$

where  $SOC(t)$  is the battery  $SOC$  at time  $t$  in %,  $SOC(t-1)$  the battery's initial  $SOC$  in %,  $t$  the time in hour,  $P$  the charge/discharge power and  $E_{bat}$  is the battery capacity.

Charging the battery with 1800 kW for 130 s makes it possible to add USD 1.95 as claimed by Vadset (2018) with a rate of USD 0.03/kWh. A separate study from Kersey *et al.* (2022) used the price of electricity of USD 0.035/kWh. This paper, however, will utilise the average value of USD 0.033/kWh. The cost to charge the battery fully after every trip will be based on the formula in equation (7),

$$Battery\ Charging_{Cost} [USD] = (SOC - SOC(t)) \times E_{bat} [kWh] \times Charging\ Cost [USD/kWh] \quad (7)$$

where  $SOC - SOC(t)$  is the percentage of battery to be fully charged,  $E_{bat}$  is the battery capacity and Charging Cost will be USD 0.033/kWh at 1800 kW. To obtain the annual operation cost with battery charging for configurations with a battery, the  $Battery\ Charging_{cost}$  is multiplied by the total number of trips completed in a year and added with  $Cost_{annual}$  in (5), not factoring downtime and inactivity periods such as system breakdown or lunch. Charging duration will progressively improve as the technology matures, evidenced by successful cases in the automobile industry where the chargers are capable of charging one vehicle at 1 MW or three vehicles simultaneously at 360 kW (Heliox, 2022).

### 3.4 CO2 Emissions

The CO<sub>2</sub> emissions  $Emission_{CO_2}$  calculation is based on MEPC.245 (66) (The Marine Environment Protection Committee, 2014). The total CO<sub>2</sub> emissions can be calculated using the following formula based on the total fuel oil consumption  $C_{fuel}$ .

$$Emission_{CO_2} (ton) = C_{fuel} (ton) \times C_F \quad (8)$$

where  $C_F$  represents the CO<sub>2</sub> emission coefficient based on the type of fuel oil consumed. The coefficients are based on MEPC.245 (66) Committee 2014. The diesel used in this paper is diesel oil and has a  $C_F$  value of 3.206, whereas the LNG has a  $C_F$  value of 2.75.

### 3.5 CII Ratings

Lastly, the  $EEOI$  or  $CII$  attained will be calculated from (9), whereas the required annual operational  $CII$  is obtained from (10).

$$EEOI \text{ or } CII \text{ attained } \left[ \frac{g}{tonne - nm} \right] = \frac{Emission_{CO_2}}{DWT \text{ or } GT [tonne] \times Distance \text{ Sailed } [nm]} \quad (9)$$

$$CII_R = aCapacity^{-c} \quad (10)$$

$$\text{Required Annual Operational } CII = \left( 1 - \frac{Z}{100} \right) \times CII_R \quad (11)$$

where  $Z$  refers to the reduction factor, starting from 5% in 2023 and afterwards increasing by 2% each year. The  $CII$  reference value  $CII_R$  (10) is based on the respective ship type and capacity from the table found in MEPC.353 (78) (The Marine Environment Protection Committee, 2022a). The values of  $a$  and  $-c$  are 930 and 0.383 respectively. The distance sailed in this study is the average distance travelled by the diesel operational tugboat of 10.4 nm. The calculated values will have a  $CII$  rating based on Table 3. The rating is based on the ratio of  $EEOI$  or  $CII$  attained (9) to the required  $CII$  (11), where a higher ratio indicates a worse rating, and vice versa. Any values lower than column B in Table 3 are rated as A (Gianni *et al.*, 2022). As tugboats are not categorised under the list of vessel types in MEPC.354 (78) (The Marine Environment Protection Committee, 2022a), this study adopts the cruise passenger ship values for  $EEOI$  calculations and  $CII$  ratings.

**Table 2 CII rating for the different types of ships** (The Marine Environment Protection Committee, 2022b)

Ship Type	Ship Size	B	C	D	E
<b>Bulk Carrier</b>		0.86	0.94	1.06	1.18
<b>Gas Carrier</b>	DWT ≥ 65,000	0.81	0.91	1.12	1.44
	DWT < 65,000	0.85	0.95	1.06	1.25
<b>Tanker</b>		0.82	0.93	1.08	1.28
<b>Container Ship</b>		0.83	0.94	1.07	1.19
<b>General Cargo Ship</b>		0.83	0.94	1.06	1.19
<b>Refrigerated Cargo Carrier</b>		0.78	0.91	1.07	1.20
<b>Combination Carrier</b>		0.87	0.96	1.06	1.14
<b>LNG Carrier</b>	DWT ≥ 100,000	0.89	0.98	1.06	1.13
	DWT < 100,000	0.78	0.92	1.10	1.37
<b>Ro-ro Cargo Ship (VC)</b>		0.86	0.94	1.06	1.16
<b>Ro-ro Cargo Ship</b>		0.76	0.89	1.08	1.27
<b>Ro-ro Passenger Ship</b>		0.76	0.92	1.14	1.30
<b>Cruise Passenger Ship</b>		0.87	0.95	1.06	1.16

## 4. RESULTS AND DISCUSSION

The results and discussion in this section are of the following cases: (I) System validation and (II) Varying environmental conditions. The types of system of configuration considered in this paper include diesel, LNG with variable engine speed and two variations of LNG-battery hybrid with control strategies. The target of the study is to first provide validity of the system model based on past operational results in Case I. This is followed by studying the different effects on the vessel load, annual operational cost and CO<sub>2</sub> emissions when different environmental conditions are encountered in Case II. The study is then concluded with a comparison of the different system configurations and highlighting the most economically friendly based on the different results and design sustainability based on CII ratings. The load profile presented in this section represents a single tugboat operation based on the system models mentioned in the System Overview.

### 4.1 Case I: System Validation with Past Operational Data

The purpose of system validation of the system modelled is to showcase the reliability and accuracy of the profiles simulated when compared to real-time operations. The load profiles used in this study are based on a combination of manually logged engine load data from past operations conducted by JMS Kappa and the designed operation load profile distribution of the LNG-battery hybrid tugboat provided by the industry collaborator. The ideal distribution of the load profile used in this study is shown in Figure 8(a). Figure 8(a), however, does not factor in the distance of the operation including the environmental conditions, as shown in Figure 5, which will affect the duration during the specified operation.

On the other hand, Table 3 breaks down the load profile given in Figure 8(a) by the operational profile by using both the manual data obtained and the duration of the stated operation provided by the industrial collaborator. Figure 8(b) however shows the results of the same input from Figure 8(a), with the consideration of the distance, environmental conditions and added resistance in AMESIM. Results show that travelling at a higher speed of 10-12 knots in Figure 8(b) requires a shorter time when compared to Figure 8(a). The breakdown of the operational profile in Figure 8(b) by its distributed duration and simulated load, is given in Table 3 where a majority of the operation is spent on tugging. The average load for Figure 8(a) is 630kW. Compared to the average load of 606kW of Figure 8(b), that factors the added resistance throughout the trip. A lower average load since more than 50% of the operation was spent tugging and requiring a load less than 550kW, reducing the overall average load. As compared to Figure 8(a) which spent 35% of the operation tugging and spent a longer duration transiting at 10-12 knots, hence the higher average load. The following study in this paper references Case I results shown in Figure 8(b) as the controlled load profile.

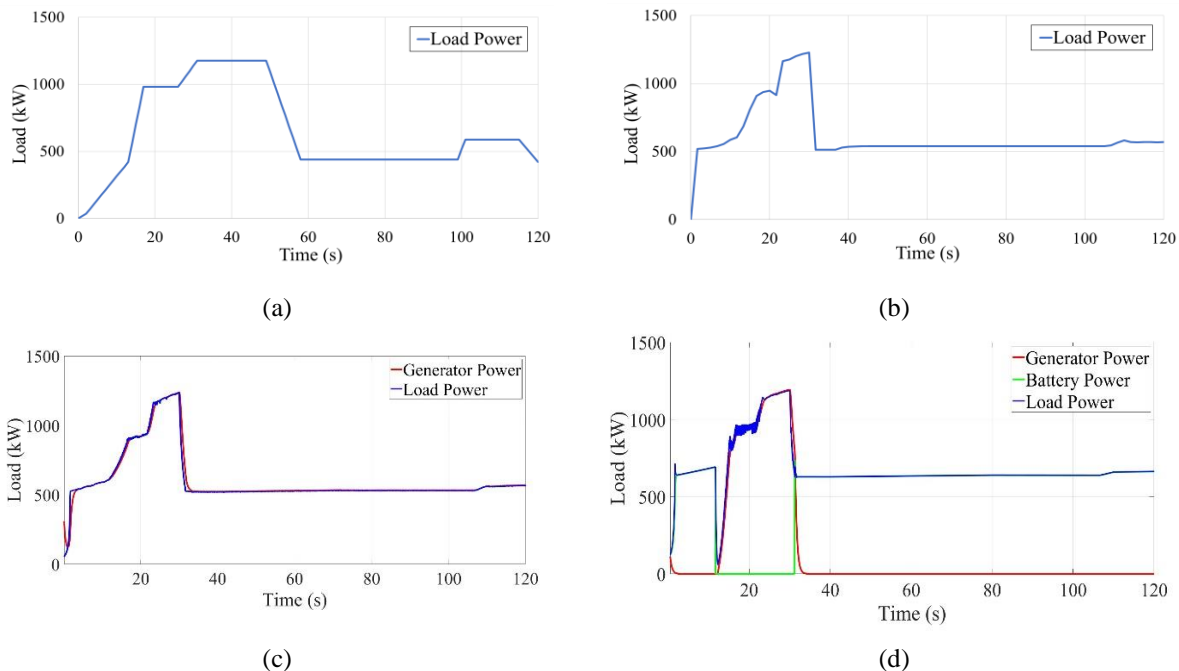


**Figure 8: (a) Load profile based on past data (b) load profile based on operational conditions (c) Load profile simulated without battery (d) Load profile simulated with battery**

Several types of system configurations such as diesel, LNG and LNG-battery hybrid with control strategies are then simulated to compare the annual cost and CO<sub>2</sub> emissions emitted based on the calculations in Section 3. Table 4 summarises the annual fuel cost and annual CO<sub>2</sub> emissions from the different system configurations. To simplify the annual calculations, no day off or downtime of the vessel throughout the year was assumed. Figure 8(c) and Figure 8(d) display the results of LNG

propulsion and LNG-battery hybrid systems on Simulink respectively. LNG-RB configuration displays the best results when compared to the other system configurations. The LNG-RB control strategy can reduce annual CO<sub>2</sub> emissions by up to 96.5% and save annual fuel operation costs of up to 95.3%. This is an improvement as compared to the results found in Roslan *et al.* (2023) because of the difference in the distribution of operation duration shown in Table 3 and the lower average load. It is worth mentioning that RB strategies will differ from study to study, it is not a one rule fits all solution. A separate RB study conducted by Diniz *et al.* (2023) controls the operational performance of the generators of an escort tug to perform at optimal efficiency and to have bi-directional battery control, which reduced CO<sub>2</sub> emissions by 10.7% for a single load profile.

Although LNG-RB results in having the best results concerning cost and emission, the number of daily trips is lesser than the conventional diesel system. This is due to the high battery usage per trip of 73.2% when compared to the other hybrid control configurations as shown in Table 4. The total number of trips completed daily is calculated based on the total duration of a day divided by the total time to complete an operation and the time to charge the battery fully. Therefore, with a higher SOC used, it will require the ship to return to port to charge after every trip. Without a bi-directional converter the battery will not be able to charge offshore, hence limiting the number of trips daily. With the current battery system configuration, the only means of charging is by connecting to shore power or swapping batteries. Therefore, with the current battery system configuration the LNG/BAT at 80% LNG and 20% battery load distribution configuration is ideal, since it consumes 16.2% SOC. A more operational-orientated configuration where a fully charged battery is capable of a single operation of up to 10 hours or five 120-minute operations, with varying loading conditions between idle, transiting and tugging up to an average of 3150kWh power consumption. While still having a reduction of annual fuel cost and CO<sub>2</sub> emissions by 65.9% and 27.7% respectively.

**Table 3 Operation Profiles**

Operation	Logged Load (kW)	Designed Duration (%)	Simulated Load (kW)	Simulated Duration (%)
Idle	420	10	521	6.9
6-knot Transit	588	25	549	26.4
10-knot Transit	980	10	927	5.6
12-knot Transit	1176	20	1083	8.3
Tugging	440	35	538	52.8

**Table 4: Case I results in comparison using different system configurations.**

Fuel Type	Annual Fuel Cost (\$USD)	Annual CO <sub>2</sub> Emission (tonne)	Battery SOC used per trip (%)	Number of trips Daily	% Reduction*	
					in Cost	in CO <sub>2</sub> Emissions
Diesel	2,571,224	8,050.1	-	12	-	-
LNG	917,906	6,245.5	-	12	64.3	22.4
LNG-RB	121,678	278.2	73.2	10	95.3	96.5
LNG/BAT (10/90)	210,632	900.8	80.1	10	91.8	88.8
LNG/BAT (20/80)	334,662	1,788.9	76.5	10	87.0	77.8
LNG/BAT (30/70)	427,341	2,480.1	66.6	11	83.4	69.2
LNG/BAT (40/60)	489,659	2,937.3	49.9	11	81.0	63.5
LNG/BAT (50/50)	551,321	3,343.0	52.6	11	78.6	58.5
LNG/BAT (60/40)	653,281	4,139.9	37.6	11	74.6	48.6
LNG/BAT (70/30)	710,903	4,594.4	29.3	11	72.4	42.9
LNG/BAT (80/20)	876,038	5,822.4	16.2	12	65.9	27.7
LNG/BAT (90/10)	1,016,854	6,851.4	7.7	12	60.5	14.9

\* concerning diesel system configuration results

## 4.2 Case II: Varying Environmental Conditions (Extreme and Operational Cases)

### 4.2.1 Loading and Energy Consumption of Battery

The four environmental conditions that investigated in this paper are based on the capabilities of the Simcenter/AMESIM module MARWAT00R, i.e., wind speed, wave height, current speed and wave period. The data are based on the data mentioned in Section 2.2 The required vessel loads of the varying extreme environmental conditions are then simulated between the minimum and maximum values based on past data experienced along the vessel route shown in Figure 5. Figure 10(a) compares the vessel load with varying wind speeds ranging between 0 m/s and 9.5m/s. An increase in the load is observed when a

variation of vessel speed is required. Significant observation can be seen at 30 – 40 minutes where a change of speed is required to accelerate back up. A surge of load is observed to increase incrementally with the wind speed. However, the average vessel load only increased by 0.93% when the wind speed increased to 9.5m/s from 0 m/s as observed from the AMESIM simulation. Table 5 summarises the comparison of the extreme results between the minimum and maximum environmental conditions. Aside from the vessel load, the vessel’s added resistance and specific fuel consumption (SFOC) are also compared using the Simcenter/AMESIM software. A decrease of 0.24% and an increase of 0.97% were observed for the average SFOC and vessel’s added resistance respectively.

A major difference could be observed when comparing the results of varying wind speeds against varying wave heights. In Figure 10(b), the vessel load of varying wave heights is shown, ranging from 0m to 5m. Notably, two key variances emerge in terms of the total time required to complete the operation and the maximum load. The total duration for completing the same operation extended from 120 minutes to 133.3 minutes, while the maximum load surged from 1228kW to 3121kW. Comparing between 0m and 5m wave heights, the average load doubled. This increase in the average vessel load led to a rise in the average vessel’s added resistance by 50.3kN, nearly seven times higher than the results obtained without considering any wave height. From past studies found in Roslan *et al.* (2023), the higher the vessel load required the lower the SFOC. A decrease of 9.6% in the average SFOC was observed due to the higher average load in general.

However, simulating extreme conditions of current speeds and wave periods produced minimal to negligible effects on the vessel load, SFOC, and added resistance. Figure 10(c) illustrates the absence of effects on the vessel when varying current speeds within the range of 0 m/s to 1.2 m/s. Additionally, Figure 10(d) depicts the variation in wave periods between 0 seconds and 9 seconds, resulting in a mere 0.06% increase in average load and a 0.80% increase in the average vessel’s added resistance observed in the AMESIM simulation (see Table 5). A summary of the findings from the varying environmental conditions is shown in Table 5, concerning the difference in percentages between the minimum and maximum results. Based on the summary Table 5, the environmental conditions that govern the loading and energy consumption of the vessel are the varying wind speeds and wave heights.

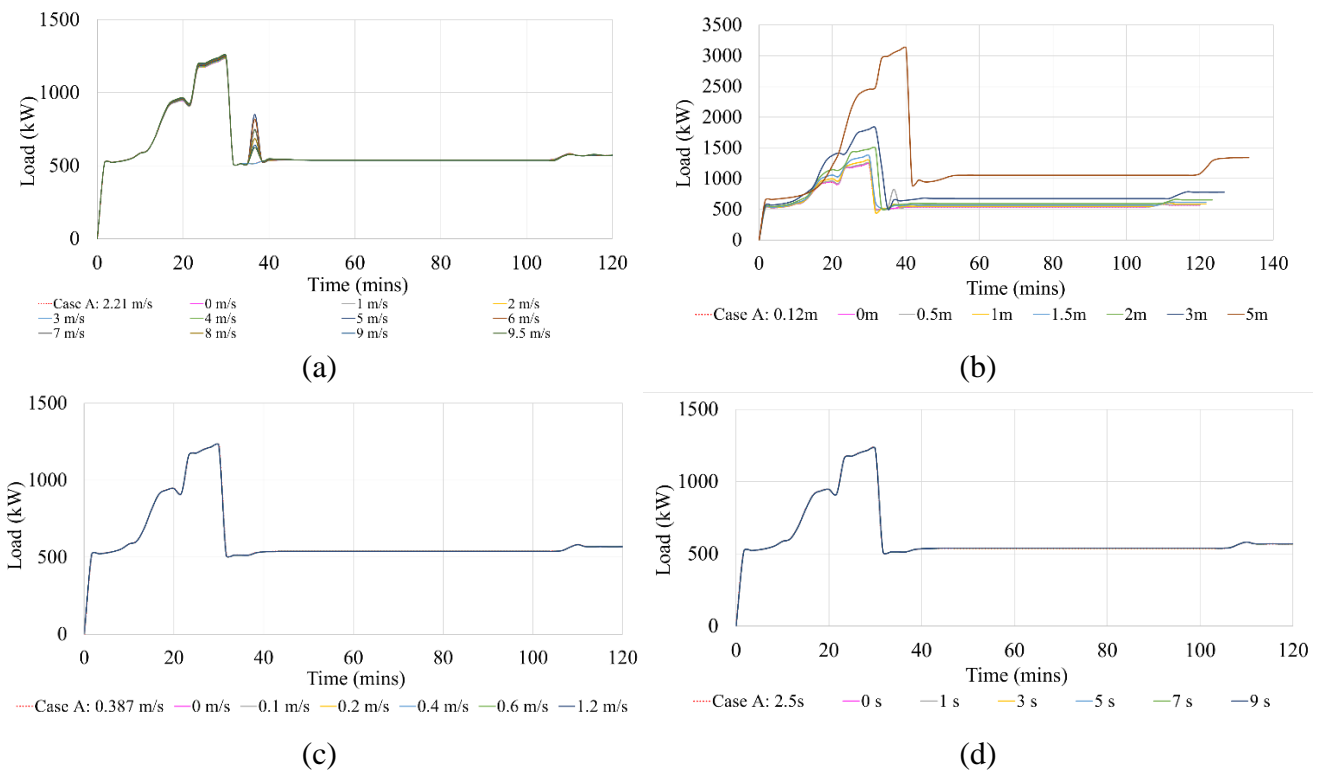


**Figure 9: Load profiles of (a) varying wind speeds (b) varying wave heights (c) varying current speeds (d) varying wave periods**

**Table 5: Results comparisons between the minimum and maximum results from varying environmental conditions**

	Wave Period	Current Speed	Wind Speed	Wave Height
<b>Load</b>	0.06%	0.00%	0.93%	104.03%
<b>SFOC</b>	-0.02%	0.00%	-0.24%	-9.62%
<b>Added Resistance</b>	0.80%	0.00%	0.97%	681.96%

#### 4.2.2 Annual Costs and CO<sub>2</sub> Emissions

Next, the study focuses on studying the average load, annual fuel operational cost and CO<sub>2</sub> emissions for the different system configurations under varying environmental conditions of the specified route. The range of values of wave heights is based on the average values obtained from past data (Windfinder, 2020) where the typical wave height along the route and around Singapore typically averages between 0.5 m and 1.0 m (Bricheno *et al.*, 2015).

The annual fuel operation cost and annual CO<sub>2</sub> emissions for the varying operational conditions under different wave heights are shown in Table 6 and Table 7, respectively. A small difference in the average load is observed between 1.0m and 0.5m wave height at 608.14kW and 608.20kW respectively. The change in speed from high speed to low speed causes the vessel's average load to be higher at 0.5m wave height. The 1.0m wave height, however, takes more time (1.67 minutes more in the simulation) to complete the operation. The results for the annual cost and annual CO<sub>2</sub> emissions are found to correlate with the increase in average load where the cost and emission increase with the increase in average load. The highest increase in the annual fuel operation cost and CO<sub>2</sub> emissions along the route due to wave heights is by 4.8% and 16.3% respectively, at 0.5m wave height using LNG-RB system configuration. This is likely due to the increase in the average load from 604.45kW to 608.20kW, although a higher load typically leads to having lower SGC. The period where the increase in load for this configuration occurred was less than 800kW, therefore 200g/kWh SGC was consumed instead of 195g/kWh resulting in a higher cost and emission.

**Table 6: Annual Cost results from varying operational wave heights**

Fuel Type	Annual Fuel Cost	Annual Fuel Cost	Annual Fuel Cost	% Increase*	
	(\$USD) – Case I*	(\$USD) – 0.5m	(\$USD) – 1m	in Cost – 0.5m	in Cost – 1m
<b>Diesel</b>	2,571,224	2,462,561	2,491,973	-4.2%	-3.1%
<b>LNG</b>	917,906	898,764	898,194	-2.1%	-2.1%
<b>LNG-RB</b>	121,678	127,459	122,973	4.8%	1.1%
<b>LNG/BAT (10/90)</b>	210,632	211,569	211,503	0.4%	0.4%
<b>LNG/BAT (20/80)</b>	334,662	336,250	336,021	0.5%	0.4%
<b>LNG/BAT (30/70)</b>	427,341	428,964	429,108	0.4%	0.4%
<b>LNG/BAT (40/60)</b>	489,659	492,029	491,428	0.5%	0.4%
<b>LNG/BAT (50/50)</b>	551,321	553,460	553,658	0.4%	0.4%
<b>LNG/BAT (60/40)</b>	653,281	656,594	656,437	0.5%	0.5%
<b>LNG/BAT (70/30)</b>	710,903	714,122	713,646	0.5%	0.4%
<b>LNG/BAT (80/20)</b>	876,038	880,555	878,759	0.5%	0.3%
<b>LNG/BAT (90/10)</b>	1,016,854	1,021,319	1,019,921	0.4%	0.3%

\* concerning respective Case I results

**Table 7: Annual CO<sub>2</sub> Emissions results from varying operational wave heights**

Fuel Type	Annual Emissions	Annual Emissions	Annual Emissions	% Increase*	
	(ton) – Case I*	(ton) – 0.5m	(ton) – 1m	in CO <sub>2</sub> Emissions – 0.5m	in CO <sub>2</sub> Emissions – 1m
<b>Diesel</b>	8,050.1	7,709.9	7,802.0	-4.2%	-3.1%
<b>LNG</b>	6,245.0	6,115.0	6,111.1	-2.1%	-2.2%
<b>LNG-RB</b>	278.2	323.5	284.3	16.3%	2.2%
<b>LNG/BAT (10/90)</b>	900.8	904.1	903.5	0.4%	0.3%
<b>LNG/BAT (20/80)</b>	1788.9	1,796.7	1,794.9	0.4%	0.3%
<b>LNG/BAT (30/70)</b>	2480.1	2,488.2	2,489.1	0.3%	0.4%

<b>LNG/BAT (40/60)</b>	2,937.3	2,950.8	2,946.3	0.5%	0.3%
<b>LNG/BAT (50/50)</b>	3,343.0	3,354.6	3,355.9	0.3%	0.4%
<b>LNG/BAT (60/40)</b>	4,139.8	4,160.3	4,159.0	0.5%	0.5%
<b>LNG/BAT (70/30)</b>	4,594.3	4,614.4	4,610.9	0.4%	0.4%
<b>LNG/BAT (80/20)</b>	5,822.4	5,852.1	5,839.5	0.5%	0.3%
<b>LNG/BAT (90/10)</b>	6,851.4	6,881.2	6,871.6	0.4%	0.3%

\* concerning respective Case I results

The operational wind speed experienced by the vessel along the route changes from 0 m/s to 9.5 m/s, as indicated by data collected from sensors on a vessel navigating the same route. Table 8 and Table 9 present the differences in annual cost and annual CO<sub>2</sub> emissions, respectively. The average load is 602.16kW at 0m/s and 606.55kW at 9.5m/s wind speed. This load is lower when compared to the impact of wave height. The increase in average wind speed along the route results in a 2.8% rise in annual fuel operation cost and a 9.4% increase in annual CO<sub>2</sub> emissions at a wind speed of 9.5m/s using the LNG-RB system configuration. The results with 0m/s wind speed are expected to be lesser in cost and emissions because Case I was simulated with an average wind speed of 2.25m/s.

**Table 8: Annual cost results comparison of varying wind speeds**

Fuel Type	Annual Fuel Cost (\$USD) – Case I*	Annual Fuel Cost (\$USD) – 0 m/s	Annual Fuel Cost (\$USD) – 9.5m/s	% Increase*	
				in Cost – 0m/s	in Cost – 9.5m/s
<b>Diesel</b>	2,571,224	2,437,919	2,453,265	-5.2%	-4.6%
<b>LNG</b>	917,906	890,217	896,355	-3.0%	-2.3%
<b>LNG-RB</b>	121,678	122,612	125,123	0.8%	2.8%
<b>LNG/BAT (10/90)</b>	210,632	210,113	211,168	-0.2%	0.3%
<b>LNG/BAT (20/80)</b>	334,662	335,652	335,647	0.3%	0.3%
<b>LNG/BAT (30/70)</b>	427,341	426,601	427,906	-0.2%	0.1%
<b>LNG/BAT (40/60)</b>	489,659	488,455	490,761	-0.2%	0.2%
<b>LNG/BAT (50/50)</b>	551,321	549,639	552,079	-0.3%	0.1%
<b>LNG/BAT (60/40)</b>	653,281	651,943	654,960	-0.2%	0.3%
<b>LNG/BAT (70/30)</b>	710,903	709,271	712,495	-0.2%	0.2%
<b>LNG/BAT (80/20)</b>	876,038	874,027	878,402	-0.2%	0.3%
<b>LNG/BAT (90/10)</b>	1,016,854	1,014,480	1,018,958	-0.2%	0.2%

\* concerning respective Case I results

**Table 9: Annual CO<sub>2</sub> emissions results comparison of varying wind speeds**

Fuel Type	Annual Emissions (ton) – Case I*	Annual Emissions (ton) – 0m/s	Annual Emissions (ton) – 9.5m/s	% Increase*	
				in CO <sub>2</sub> Emissions – 0m/s	in CO <sub>2</sub> Emissions – 9.5m/s
<b>Diesel</b>	8,050.1	7,632.8	7,680.8	-5.2%	-4.6%
<b>LNG</b>	6,245.5	6,057.1	6,098.9	-3.0%	-2.3%
<b>LNG-RB</b>	278.2	285.7	304.3	2.7%	9.4%
<b>LNG/BAT (10/90)</b>	900.8	899.1	902.6	-0.2%	0.2%
<b>LNG/BAT (20/80)</b>	1788.9	1,798.2	1,793.8	0.5%	0.3%
<b>LNG/BAT (30/70)</b>	2480.1	2,476.9	2,482.0	-0.1%	0.1%
<b>LNG/BAT (40/60)</b>	2,937.3	2,930.7	2,943.1	-0.2%	0.2%
<b>LNG/BAT (50/50)</b>	3,343.0	3,333.0	3,346.2	-0.3%	0.1%
<b>LNG/BAT (60/40)</b>	4,139.9	4132.2	4,149.9	-0.2%	0.2%
<b>LNG/BAT (70/30)</b>	4,594.4	4584.4	4,603.9	-0.2%	0.2%
<b>LNG/BAT (80/20)</b>	5,822.4	5809.4	5,837.8	-0.2%	0.3%
<b>LNG/BAT (90/10)</b>	6,851.4	6835.6	6,865.4	-0.2%	0.2%

\* concerning respective Case I results

In summary, the results summarised in Table 5 show the extreme results for load, SFOC and added resistance between the minimum and maximum environmental conditions. Varying wave heights are found to have the highest effect on the results followed by varying wind speed. The results from varying operational wave heights show an increase of up to 4.8% and 16.4% in the annual fuel operation cost and annual CO<sub>2</sub> emissions, respectively. As for the varying operational wind speeds, an increase of up to 2.8% and 9.4% in the annual fuel operation cost and annual CO<sub>2</sub> emissions, respectively. Additionally, different system configurations were tested. Similar to Case I, the LNG-RB configuration demonstrated the most significant reduction in cost and emissions when compared to the diesel configuration. The capabilities of the system model used in this study to simulate the effects of environmental loads to the system performance will be beneficial for vessel operator or machine learning algorithms. Algorithms such as route optimisation-based solutions based on the most efficient conditions discovered in this paper. Having knowledge of which environmental conditions to avoid will save valuable operational cost and emissions.

### 4.3 Economical and Sustainability System Comparison

With the results of the different system configurations in Case I and Case II, the CII ratings of the respective system are then calculated using the equations (9) – (11) expressed in Section 3. Table 10 summarises the results of the CII ratings for the following years based on the results simulated. Achieving a grade “A” CII rating signifies a highly efficient ship in reducing carbon emissions during operation. With future readiness for a more environmentally friendly maritime industry. Vessel designs with a score of “D” or “E” for three consecutive years are required to develop a corrective action plan. Based on the CII ratings of the configuration tested, it is highly recommended that the vessels operate with at least 30% of the load with battery and 70% on LNG. Operating on diesel and LNG is not recommended since it is the least efficient with a grade “E” CII rating.

**Table 10: CII Ratings of the respective configurations through the years**

Configuration \ Year	2024	2025	2026	2027
Diesel	E	E	E	E
LNG	E	E	E	E
LNG-RB	A	A	A	A
LNG/BAT (10/90)	A	A	A	A
LNG/BAT (20/80)	A	A	A	A
LNG/BAT (30/70)	A	A	A	A
LNG/BAT (40/60)	A	A	A	A
LNG/BAT (50/50)	A	A	A	B
LNG/BAT (60/40)	A	B	C	D
LNG/BAT (70/30)	B	C	D	E
LNG/BAT (80/20)	D	E	E	E
LNG/BAT (90/10)	E	E	E	E

Although the CII ratings play a big part in selecting a system configuration with efficient carbon emission and sustainability, the reality in operation is to have a system design capable of providing both efficiency in completing more operations and in reducing emissions. LNG-RB demonstrated the best in performance with the biggest reduction in annual fuel operation cost and annual CO<sub>2</sub> emission and obtained a grade “A” CII rating. However, the total number of trips capable of completing within a day is limited to 10 trips as compared to the 11 trips using a 30% LNG and 70% battery load distributed system. The single increase in operation leads to an increase in the annual fuel operation cost and CO<sub>2</sub> emissions by \$USD 305,663 and 2,202 tons, respectively. It is imperative, therefore, to refrain from increasing the trip count to 11, and instead allocate the extra time for battery charging due to the significant surge in costs and emissions. With the cost saved, an enhancement to the configuration could involve incorporating a bi-directional converter due to their electrical isolation capabilities and high reliability in renewable energy sources (Dung *et al.*, 2017), and also enabling the battery to be charged by the LNG generators onboard.

The annual fuel operation cost and CO<sub>2</sub> emissions results from this paper could be used for a further study on the life cycle assessment (LCA) and life cycle cost assessment (LCCA) of the LNG-battery hybrid system model. A similar study done by Fan *et al.* (2021) where the economic and environmental impact of the lifetime of a LNG-battery hybrid river ship was assessed and compared to a diesel propulsion. The annual emissions reduced by 33.44% and fuel cost reduced by 39.15%, including carbon emission tax, when compared between the LNG-battery hybrid to diesel system. For future LCA assessment on CO<sub>2</sub> emissions, factors to consider include but not limited to the following: emission during equipment manufacturing stage, energy production stage and energy transportation. For LCCA on the other hand considers the total cost including investment cost,

operation cost (maintenance cost, fuel cost and carbon credit cost) and decommission cost. The results from Fan's LCCA concluded with LNG-battery hybrid system costing less than the diesel-powered system. Future works alternative tugboats propulsion systems should consider comparing different renewable energies such as methanol and hydrogen. A similar work had been done by Perčić *et al.* (2021), where he investigated on the LCA and LCCA of various ships using alternative fuels. The study concluded with fully electric ships being the most environmentally and cost-effective solution, followed closely by methane and LNG. A similar study could be conducted in the near future for tugboats with the results obtained from the current study which will benefit potential vessel owners before converting current diesel systems to an alternative renewable energy propulsion system.

## 5. CONCLUSIONS

The paper presented the influence of environmental loads and manoeuvre on the vessel load in several different system configurations. The configurations include a full diesel system, LNG system, LNG-battery hybrid system with rule-based control and LNG-battery hybrid system with flexible load sharing. The annual fuel operation cost, annual CO<sub>2</sub> emissions and CII ratings for each system configuration at the varying environmental load were calculated and discussed in the paper. The cases covered in this paper are as follows: Case I: System Validation and Case II: Varying environmental conditions. Case I validates the system modelled with past results manually captured from similar tugboats. The model was created on Siemen/AMESIM for the diesel system configuration and MATLAB/Simulink for the LNG and LNG-battery hybrid systems. The LNG-RB system showcased its capabilities with the lowest annual fuel operation cost and annual CO<sub>2</sub> emissions when compared to the conventional diesel system with a reduction of 95.3% and 96.5% respectively.

The results in Case I were set as a benchmark when compared to results from Case II with the varying environmental conditions. The conditions included in the study are wind speed, wave height, current speed and wave periods. Each environmental condition was tested between zero and the extreme condition experienced through the route. The results concluded that wave height had the biggest impact on the vessel load performance, with an average increase of 104.03% and 681.96% in load and added resistance respectively. The varying wind speed displayed a slight increase in the load and added resistance, unlike the varying current speed and wave periods that had no impact on the vessel's performance. The wave height and wind speed are then simulated using operational conditions to calculate the respective annual fuel operational cost and annual CO<sub>2</sub> emissions. The operational wave height along the route ranges between 0.5m and 1m. An increase of up to 4.8% and 16.3% to the annual fuel operational cost and CO<sub>2</sub> emissions when compared to Case I results. The operational wind speed experience along the route simulated ranges between 0 m/s to 9.5m/s . An increase of up to 2.8% and 9.4% in annual fuel operational cost and CO<sub>2</sub> emissions can be obtained between extreme wind speed and average wind speed at 2.25 m/s.

The paper concludes with the CII ratings of each system configuration to find the most efficient system for reducing emissions. LNG-RB and LNG/RB load sharing with more than 40% battery load had the best CII rating of grade "A". However, based on the number of daily trips capable of completing with a fully charged battery, LNG-RB was limited to 10 trips whereas LNG/RB with 30% LNG and 70% battery load sharing was able to complete 11 trips. The annual increase in cost and emission for the additional trip increased by \$USD 305,663 and 2,202 tons, respectively. Therefore, it is more economical and efficient to maintain 10 trips using LNG-RB system configuration. Using the allowance of time to travel back to shore for charging or battery swap. Moreover, the funds designated for this purpose could be redirected to enhance the vessel system by integrating a bi-directional converter. This converter facilitates better control over the battery's voltage and current, crucially enabling offshore charging by the LNG generators. To enhance the credibility of the modelled system, future investigations should encompass a broader range of case studies, including diverse routes and varying operational vessel loads. Subsequent studies could involve integrating live sensor data into the model to create a digital twin capable of producing route optimisation and load predictions.

## CONTRIBUTION STATEMENT

**Sharul Baggio Roslan:** Conceptualization, methodology, data collection, validation, writing – original draft preparation, data collection, visualization. **Dimitrios Konovessis:** supervision, funding acquisition. **Joo Hock Ang:** validation, data collection. **Nirmal Vineeth:** validation, data collection. **Zhi Yung Tay:** methodology, writing – review and editing, supervision, project administration, funding acquisition.

## ACKNOWLEDGEMENTS

This research was funded by MOE, Grant Number R-MOE-A403-E002.

## REFERENCES

- Abebe, M., Shin, Y., Noh, Y., Lee, S., & Lee, I. (2020). Machine learning approaches for ship speed prediction towards energy efficient shipping. *Applied Science*, 10(7), 2325.
- Bricheno, L., Cannaby, H., Howard, T., McInnes, K., & Palmer, M. (2015). Extreme Sea Level Projections. *Centre for Climate*

*Research Singapore.*

- Cheliotis, M., Lazakis, I., & Theotokatos, G. (2020). Machine learning and data-driven fault detection for ship systems operations. *Ocean Engineering*, 216(May), 107968. <https://doi.org/10.1016/j.oceaneng.2020.107968>
- Chua, L. W. Y. (2019). *A Strategy for Power Management of Electric Hybrid Marine Power Systems* [Nanyang Technological University]. <https://doi.org/10.32657/10220/48078>
- ClassNK. (2021). *Outlines of EEXI regulation EEDI Section of Marine GHG Certification Department*. [https://www.classnk.or.jp/hp/pdf/activities/statutory/eexi/eexi\\_rev3e.pdf](https://www.classnk.or.jp/hp/pdf/activities/statutory/eexi/eexi_rev3e.pdf)
- Diniz, G. H. S., Miranda, V. dos S., & Carmo, B. S. (2023). Dynamic modelling, simulation, and control of hybrid power systems for escort tugs and shuttle tankers. *Journal of Energy Storage*, 72, 108091. <https://doi.org/10.1016/J.EST.2023.108091>
- Dung, N. A., Hieu, P. P., Hsieh, Y., Lin, J., Liu, Y., & Chiu, H. (2017). A novel low-loss control strategy for bidirectional DC–DC converter [Article]. *International Journal of Circuit Theory and Applications*, 45(11), 1801–1813. <https://doi.org/10.1002/cta.2373>
- Ejder, E., & Arslanoğlu, Y. (2022). Evaluation of ammonia fueled engine for a bulk carrier in marine decarbonization pathways [Article]. *Journal of Cleaner Production*, 379. <https://doi.org/10.1016/j.jclepro.2022.134688>
- Fam, M. L., Tay, Z. Y., & Konovessis, D. (2022). An artificial neural network for fuel efficiency analysis for cargo vessel operation. *Ocean Engineering*, 264, 112437. <https://doi.org/10.1016/J.OCEANENG.2022.112437>
- Fan, A., Wang, J., He, Y., Perčić, M., Vladimir, N., & Yang, L. (2021). Decarbonising inland ship power system: Alternative solution and assessment method. *Energy*, 226, 120266. <https://doi.org/10.1016/J.ENERGY.2021.120266>
- Gianni, M., Pietra, A., Coraddu, A., & Taccani, R. (2022). Impact of SOFC Power Generation Plant on Carbon Intensity Index (CII) Calculation for Cruise Ships [Article]. *Journal of Marine Science and Engineering*, 10(10), 1478. <https://doi.org/10.3390/jmse10101478>
- Hadi, J., Konovessis, D., & Tay, Z. Y. (2022a). Achieving fuel efficiency of harbour craft vessel via combined time-series and classification machine learning model with operational data. *Maritime Transport Research*, 3, 100073. <https://doi.org/10.1016/J.MARTRA.2022.100073>
- Hadi, J., Konovessis, D., & Tay, Z. Y. (2022b). Filtering harbor craft vessels' fuel data using statistical, decomposition, and predictive methodologies. *Maritime Transport Research*, 3, 100063. <https://doi.org/https://doi.org/10.1016/j.martra.2022.100063>
- Hansen, J. F. (2000). *Modelling and Control of Marine Power Systems*. Norwegian University of Science and Technology.
- Heliox. (2022). *The Future is Megawatt Charging*. Heliox. <https://www.heliox-energy.com/blog/the-future-is-megawatt-charging>
- IHI. (2022). *Niigata Marine Selection Guide*. <https://www.ihl.co.jp/ips>
- IndexMundi. (2022). *Natural Gas vs Diesel - Price Rate of Change Comparison*. <https://www.indexmundi.com/commodities/?commodity=natural-gas&currency=sgd&commodity=diesel>
- International Maritime Organisation. (2019). *The 2020 global sulphur limit: FAQ*. International Maritime Organization. [http://www.imo.org/en/MediaCentre/HotTopics/GHG/Documents/FAQ\\_2020\\_English.pdf](http://www.imo.org/en/MediaCentre/HotTopics/GHG/Documents/FAQ_2020_English.pdf)
- International Maritime Organization. (2016). *Prevention of Air Pollution from Ships*. International Maritime Organization. <https://www.imo.org/en/OurWork/Environment/Pages/Air-Pollution.aspx>
- ISO. (2015). ISO 15016:2015 - Ships and marine technology — Guidelines for the assessment of speed and power performance by analysis of speed trial data. In ISO. <https://www.iso.org/standard/61902.html>
- ITTC. (2021). ITTC-Recommended Procedures and Guidelines. *International Towing Tank Conference*.
- Karaçay, Ö. E., & Özsoysal, O. A. (2021). Techno-economic investigation of alternative propulsion systems for tugboats [Article]. *Energy Conversion and Management*, 216, 100140. <https://doi.org/10.1016/j.ecmx.2021.100140>
- Kersey, J., Popovich, N. D., & Phadke, A. A. (2022). Rapid battery cost declines accelerate the prospects of all-electric interregional container shipping. *Nature Energy* 2022 7:7, 7(7), 664–674. <https://doi.org/10.1038/s41560-022-01065-y>
- Lebedevas, S., Norkevičius, L., & Zhou, P. (2021). Investigation of Effect on Environmental Performance of Using LNG as Fuel for Engines in Seaport Tugboats. *Journal of Marine Science and Engineering* 2021, Vol. 9, Page 123, 9(2), 123. <https://doi.org/10.3390/JMSE9020123>
- Lindstad, H., Asbjørnslett, B. E., & Jullumstrø, E. (2013). Assessment of profit, cost and emissions by varying speed as a function of sea conditions and freight market. *Transportation Research Part D: Transport and Environment*, 19, 5–12. <https://doi.org/10.1016/J.TRD.2012.11.001>
- Mallouppas, G., & Yfantis, E. A. (2021). Decarbonization in Shipping Industry: A Review of Research, Technology Development, and Innovation Proposals. *Journal of Marine Science and Engineering* 2021, Vol. 9, Page 415, 9(4), 415. <https://doi.org/10.3390/JMSE9040415>
- Maritime & Port Authority of Singapore. (2020). *Singapore Tide Tables*. <https://www.mpa.gov.sg/who-we-are/newsroom-resources/publications/singapore-tide-tables>
- Maritime & Port Authority Of Singapore. (2023). *Strengthening Singapore's Competitiveness as a Hub Port and International*

- Maritime Centre. <https://www.mpa.gov.sg/media-centre/details/strengthening-singapore-s-competitiveness-as-a-hub-port-and-international-maritime-centre>
- Mirović, M., Miličević, M., & Obradović, I. (2018). Big data in the maritime industry. *NAŠE MORE: Znanstveni Časopis Za More i Pomorstvo*, 65(1), 56–62.
- Moreno, V. M. (2007). Future trends in electric propulsion systems for commercial vessels. *Journal of Maritime Research*, 4(2), 81–100.
- Perčić, M., Vladimir, N., & Fan, A. (2021). Techno-economic assessment of alternative marine fuels for inland shipping in Croatia. *Renewable and Sustainable Energy Reviews*, 148, 111363. <https://doi.org/10.1016/j.rser.2021.111363>
- Roslan, S. B., Konovessis, D., Ang, J. H., Menon, N. V., & Tay, Z. Y. (2023). Modelling and Operation of a Hybrid LNG Propulsion Tugboat. *Volume 5: Ocean Engineering*. <https://doi.org/10.1115/OMAE2023-100911>
- Roslan, S. B., Konovessis, D., & Tay, Z. Y. (2022). Sustainable Hybrid Marine Power Systems for Power Management Optimisation: A Review. *Energies* 2022, Vol. 15, Page 9622, 15(24), 9622. <https://doi.org/10.3390/EN15249622>
- Roslan, S. B., Tay, Z. Y., Konovessis, D., Ang, J. H., & Menon, N. V. (2023). Rule-Based Control Studies of LNG–Battery Hybrid Tugboat. *Journal of Marine Science and Engineering* 2023, Vol. 11, Page 1307, 11(7), 1307. <https://doi.org/10.3390/JMSE11071307>
- Ship&Bunker. (2023). *Singapore Bunker Prices - Ship & Bunker*. <https://shipandbunker.com/prices/apac/sea/sg-singapore#MGO>
- Ship Technology. (2015, June 1). *Ampere Electric-Powered Ferry*. Ship Technology. <https://www.ship-technology.com/projects/norled-zero-cat-electric-powered-ferry/>
- Tadros, M., Ventura, M., & Soares, C. G. (2023). Review of current regulations, available technologies, and future trends in the green shipping industry. *Ocean Engineering*, 280, 114670. <https://doi.org/10.1016/J.OCEANENG.2023.114670>
- Tay, Z. Y.; Hadi, J; Konovessis, D.; Loh, D. J.; Tan, D. K. H; Chen, X. (2021). Efficient harbour craft monitoring system: Time-series data analytics and machine learning tools to achieve fuel efficiency by operational scoring system. *Proceedings of the ASME 2021 40th International Conference on Ocean, Offshore and Arctic Engineering OMAE 2021*, OMAE2021-62658.
- Tay, Z. Y., Hadi, J., Chow, F., Loh, D. J., & Konovessis, D. (2021). Big Data Analytics and Machine Learning of Harbour Craft Vessels to Achieve Fuel Efficiency: A Review. *Journal of Marine Science and Engineering* 2021, Vol. 9, Page 1351, 9(12), 1351. <https://doi.org/10.3390/JMSE9121351>
- Tay, Z. Y., & Konovessis, D. (2023). Sustainable energy propulsion system for sea transport to achieve United Nations sustainable development goals: a review. *Discover Sustainability*, 4(1). <https://doi.org/10.1007/S43621-023-00132-Y>
- The Marine Environment Protection Committee. (2014). *Resolution MEPC.245(66)-2014 Guidelines on the Method of Calculation of the Attained Energy Efficiency Design Index (EEDI) for New Ships*. [https://www.wcdn.imo.org/localresources/en/OurWork/Environment/Documents/245\(66\).pdf](https://www.wcdn.imo.org/localresources/en/OurWork/Environment/Documents/245(66).pdf)
- The Marine Environment Protection Committee. (2021). *Resolution MEPC.328(76) - Amendments to the Annex of the Protocol of 1997 to Amend the International Convention for the Prevention of Pollution from Ships 1973, As Modified by the Protocol of 1978 Relating Thereto 2021 Revised MARPOL Annex VI*. [https://www.wcdn.imo.org/localresources/en/OurWork/Environment/Documents/Air pollution/MEPC.328\(76\).pdf](https://www.wcdn.imo.org/localresources/en/OurWork/Environment/Documents/Air%20pollution/MEPC.328(76).pdf)
- The Marine Environment Protection Committee. (2022a). *Resolution MEPC.353 (78) - 2022 Guidelines on the Reference Lines for Use with Operational Carbon Intensity Indicators (CII Reference Lines Guidelines, G2)*. [https://www.wcdn.imo.org/localresources/en/OurWork/Environment/Documents/Air pollution/MEPC.353\(78\).pdf](https://www.wcdn.imo.org/localresources/en/OurWork/Environment/Documents/Air%20pollution/MEPC.353(78).pdf)
- The Marine Environment Protection Committee. (2022b). *Resolution MEPC.354(78) - 2022 Guidelines on the Operational Carbon Intensity Rating of Ships (CII Rating Guidelines, G4)*. [https://www.wcdn.imo.org/localresources/en/OurWork/Environment/Documents/Air pollution/MEPC.354\(78\).pdf](https://www.wcdn.imo.org/localresources/en/OurWork/Environment/Documents/Air%20pollution/MEPC.354(78).pdf)
- Turk, A., & Prpić-Oršić, J. (2009). *ESTIMATION OF EXTREME WIND LOADS ON MARINE OBJECTS Anton TURK I Jasna PRPIĆ-ORŠIĆ 2 Estimation of Extreme Wind Loads on Marine Objects*. 2, 147–156.
- Vadset, M. S. (2018). *Modeling and operation of hybrid ferry with gas engine, synchronous machine and battery*. Norwegian University of Science and Technology.
- Wang, Z., Chen, L., Wang, B., Huang, L., Wang, K., & Ma, R. (2023). Integrated optimization of speed schedule and energy management for a hybrid electric cruise ship considering environmental factors. *Energy*, 282, 128795. <https://doi.org/10.1016/J.ENERGY.2023.128795>
- Windfinder. (2020, May). *Wind, waves, weather & tide forecast Sembawang*. <https://www.windfinder.com/forecast/sembawang>
- Zahedi, B., Norum, L. E., & Ludvigsen, K. B. (2014). Optimized efficiency of all-electric ships by dc hybrid power systems. *Journal of Power Sources*, 255, 341–354. <https://doi.org/10.1016/J.JPOWSOUR.2014.01.031>